Research Article Vol. 3, No. 6 / 15 June 2020 / OSA Continuum 1385

Modifications of effective optical properties of a-Si:H/a-SiN$_x$:H multilayers by means of multilayer design and sublayer thickness

JARMILA MÜLLEROVÁ,[1,*] PAVEL ŠUTTA,[2] PAVEL CALTA,[2] MARIE NETRVALOVÁ,[2] AND ROSTISLAV MEDLÍN[2]

[1] *Institute of Aurel Stodola, Faculty of Electrical Engineering and Information Technologies, University of Žilina, ul. kpt. J. Nálepku 1390, 031 01 Liptovský Mikuláš, Slovakia*
[2] *New Technologies – Research Centre, University of West Bohemia, Univerzitní 8, 306 14 Plzeň, Czech Republic*
[*] *jarmila.mullerova@feit.uniza.sk*

Abstract: This paper presents a study of optical properties of two series of PECVD deposited planar a-Si:H/a-SiN$_x$:H multilayers that are differently arranged. The first series design is symmetric consisting of samples with equidistant a-Si:H and a-SiN$_x$:H sublayers of increasing thickness. In the second asymmetric series the thickness of a-SiN$_x$:H sublayers remains constant and the thickness of a-Si:H sublayers changes to represent materials with changing a-Si:H/a-SiN$_x$:H content ratio. From transmittance measurements refractive indices, absorption coefficients and optical band gaps were extracted and compared. The importance of the knowledge of wavelength-dependent refractive indices and absorption coefficients was demonstrated in the calculations of the absorptance under the Yablonovitch limit and of total relative absorbed solar energy. The total absorbed solar energy was commented with respect to a specific multilayer design.

1. Introduction

Silicon/silicon nitride and silicon oxide/silicon nitride stacks are generally agreed to provide a successful optical platform for high index wide band gap photonics used in LEDs, dielectric Bragg reflectors (DBR), multiplexers, optical filters, optical sensors, grating couplers, solar cells etc. [1–6]. Complex systems of solar cells with amorphous, polycrystalline or nanoparticles embedded multilayer structure have been investigated for their ability to control light transmission and reflection [7–9]. Multilayers composed from amorphous hydrogenated silicon (a-Si:H) and amorphous hydrogenated silicon nitride (a-SiN$_x$:H) belong to a wide family of silicon based representatives with variety of photonics applications [10]. Among them all silicon stacked solar cells with a multilayer as a solar absorber in which a less strongly absorbing material is accompanied with a stronger absorber [9,11] or surface passivating structures [12] must be mentioned. This concept enables engineering and optimization of optical properties of the whole structure, mainly the spectral absorption response, the band gap and the refractive index.

The knowledge of the refractive index of a solar cell absorber is important for the consideration of the optical path length, the enhancement of which is important for increasing the absorption of light. Particular progress in this enhancement can be achieved by light trapping structures with different degrees of randomness or order [13–15]. However for such light-trapping schemes there is an upper limit to increase the optical path length and the absorption known as the Yablonovitch limit referred to as $4n^2$ (where n is the refractive index) expressing the maximum increase of the optical path length [16,17]. Although this expression is generally valid for a specific geometry, it is widely accepted as an appropriate benchmark to compare various solar cell materials and concepts.

#389612 https://doi.org/10.1364/OSAC.389612
Journal © 2020 Received 3 Feb 2020; revised 24 Apr 2020; accepted 25 Apr 2020; published 27 May 2020

OSA CONTINUUM

SiN_x is considered a high refractive index (still lower than a-Si:H) and high band gap material [18–20]. Optical properties, namely refractive indices and optical band gaps are expected to be engineered when low band gap a-Si:H as a well layer is accompanied with high band gap a-SiN_x:H as a barrier layer in a multilayer structure.

Here we present a study of optical properties of planar intrinsic a-Si:H/a-SiN_x:H multilayers that differ by the thickness of sublayers and by the multilayer design. Two thickness series of multilayers deposited by two PECVD deposition systems and by slightly different deposition conditions were available. The main purpose was to investigate optical properties of multilayers within one series, and to identify possible correlations with the second series. As multilayers of this kind can play the role of an absorber in a-Si:H solar cells or due to a different optical band gap the role of a corresponding cell in a tandem cell structure, the overall multilayer thickness should correspond to a typical thickness of intrinsic a-Si:H in p-i-n thin film solar cells (300–500 nm). Refractive indices and absorption coefficients were extracted from transmittance measurements, compared and used for the calculations of the absorptance under the Yablonovitch limit of total relative absorbed solar energy.

2. Experiment

Two series of differently arranged intrinsic a-Si:H/a-SiN_x:H multilayer (ML) structures were analyzed and compared (Fig. 1). Both series were designed with a specific sublayer thickness anticipated by the adjustment of the deposition times. The first series labeled as SYM consists of samples with periodic equal-thickness alternation of a-Si:H and a-SiN_x:H, i.e. of symmetric (equal thickness) bilayers of a-Si:H/ a-SiN_x:H. In the second series labeled as ASYM periodically alternating a-Si:H and a-SiN_x:H sublayers are of unequal thickness, i.e. they are composed of asymmetric (unequal thickness) bilayers of a-Si:H/ a-SiN_x:H. The number of bilayers differs in individual members of the series so that the total thickness is comparable with conventional thicknesses of a-Si:H single thin film solar absorbers. Therefore the thickness of several nanometers was selected as the minimal thickness of individual a-Si:H sublayers and the rest of the series have some additive thicknesses.

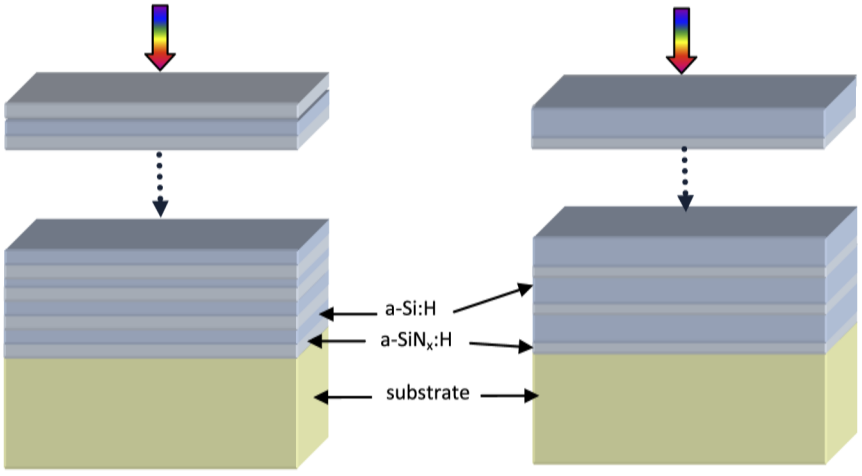

Fig. 1. Schematics of SYM (left) and ASYM multilayer structures (right).

Symmetric (SYM) multilayers composed of equidistant sublayers were deposited on quartz substrates by a capacitively coupled rf (13.56 MHz, 40 W) plasma-enhanced chemical vapor (PECVD) SAMCO 220 N parallel planar deposition system using SiH_4 (10% diluted in Ar)

OSA CONTINUUM

and N_2 as precursor gases. Working pressure was of 67 Pa and substrate temperature of 250°C. By changing the gas flow ratio $R = N_2/SiH_4$ and plasma interruption, SYM multilayer structure of alternating layers of a-Si:H (deposited from pure SiH_4 at $R = 0$) and a-SiN_x:H ($R = 120$) was deposited. The deposition was performed at the University of West Bohemia, Czech Republic, as a part of an extended study of as-deposited and annealed ML series. The deposited a-SiN_x:H sublayers were non-stoichiometric with slight Si excess content. The stoichiometric ratio $x = [N]/[Si] \approx 0.9$ was determined from the refractive index ≈ 1.92 [21] of an a-Si:N_x:H thin film deposited under identical deposition conditions and under the gas flow ratio ($R = 120$) and by the empiric formula [22] .

To deposit the sublayers of different thickness, different deposition times were used [23]. SYM ML structures denoted as SYM5, SYM10, SYM15 and SYM20 were composed of alternating uniformly thick (5, 10, 15 or 20 nm) sublayers of a-SiN_x:H and a-Si:H followed by a final a-SiN_x:H capping sublayer. No post-deposition treatment was applied.

The overall thickness was designed to be approximately constant for different ML samples. The final SYM structure was further considered as one effective monolayer. To avoid the thickness effect of this effective monolayer, the total ML thickness of all four structures was approximately the same with estimated total a-Si:H thickness of ~ 300 nm. Therefore the number of sublayers must differ (Table 1). The total thickness ratio of a-Si:H/a-SiN_x:H remains unchanged. According to TEM cross-sectional images (Fig. 2), the achieved sublayer thickness was due to PECVD deposition aspects reduced in comparison with expected (the 2nd column, Table 1). Then the thickness of final ML structures determined by KLA-Tencor P-6 Surface Profiler is less than anticipated (Table 1).

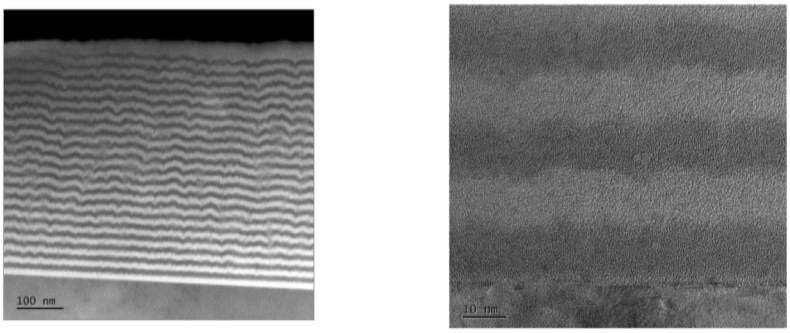

Fig. 2. Dark field (left) and bright filed (right) TEM cross-sectional images of SYM15 sample.

Table 1. Characterization of SYM samples, total thickness by UV Vis is the value from fitting the transmittance spectrum (Section 3.1).

Sample	a-Si:H layer thickness (nm)	Total number of sublayers	Total thickness by profiler (nm)	Total thickness by UV Vis (nm)
SYM5	5	121	521	512
SYM10	10	61	520	486
SYM15	15	41	520	516
SYM20	20	31	534	518

Asymmetric multilayers (ASYM) were deposited on Corning Eagle 2000 glass from SiH_4+NH_3 gas mixture in a capacitively coupled rf deposition system at TU Delft, the Netherlands [11]. Sublayers of a-SiN_x:H were deposited using 80% NH_3 in the total gas mixture. The films were deposited at an rf power density of 34 mW/cm^2, an inter-electrode distance of 14 mm, a

OSA CONTINUUM

deposition pressure of 80 Pa and a substrate temperature of 235°C. ML structures were fabricated by alternating deposition of a-Si:H well and non-stoichiometric a-SiN_x:H barrier layers ($x \approx 1$ [11]). ML structures were grown in a continuous manner, i.e. the plasma was not switched off in between the deposition of subsequent sublayers. Individual a-Si:H sublayer thicknesses varied between 1 and 25 nm. In this way the average composition of the different ML samples and the number of interfaces do not remain the same. ASYM notification in Table 2 contains the number that is the rounded thickness of a-Si:H sublayer in the ML structure. No post-deposition treatment was applied, too. A similar conclusion as in case of SYM series related to the reduced overall ML thickness in comparison with expected is valid, too.

Table 2. Characterization of ASYM samples, total anticipated thickness was calculated from the number of a-Si:H and a-SiN_x:H sublayers and their anticipated thickness (columns 4, 6), total thickness by UV Vis is the value from fitting the transmittance spectrum (Section 3.1).

Sample	Total thickness by UV Vis/total anticipated thickness (nm)	Total # of sublayers	a-Si:H layer thickness (nm)	# of a-Si:H layers	a-SiN_x:H thickness (nm)	a-SiN_x:H/a-Si:H total thickness ratio
ASYM1	438/351	137	1.3	68	3.8	2.90
ASYM3	402/349	101	3.1	50	3.8	1.05
ASYM5	359/341	75	5.3	37	3.8	0.73
ASYM10	323/323	47	10.1	23	3.8	0.39
ASYM25	335/317	23	24.7	11	3.8	0.17

Transmission electron microscopy (TEM) investigations were performed on Jeol JEM 2200FS for SYM samples. Some internal undulation can be seen in TEM image of SYM15 sample (Fig. 2). No transition layers were detected in SYM samples by TEM, XRD and AES measurements. According to TEM studies of ASYM multilayers, transition layers of ~ 1 nm can be expected [11].

The microstructure of SYM samples deposited on c-Si and ASYM samples on Corning glass was studied by X-ray diffraction analysis (XRD) using an automatic powder diffractometer X'Pert Pro with the thin film configuration (fixed and small incident angle, asymmetric geometry) and ultra-fast semiconductor detector PixelPIXcel and CuKa characteristic radiation ($\lambda = 0.154$ nm). Broad XRD patterns confirm the amorphous structure of all samples of both series (Fig. 3) in the contrary of c-Si pattern of the substrate (left).

The optical transmittance at nearly normal incidence was recorded by UV-VIS spectrophotometer Specord 210 in the range of 190 – 1100 nm with blank air reference channel. Recorded spectra are in Fig. 4. For the comparison the transmittance of a single a-Si:H thin film of the comparable thickness ~ 400 nm deposited under the same conditions as SYM samples is included in Fig. 4 (left) [24] and the one of the thickness ~ 300 nm deposited comparably as ASYM samples (right) [25]. Apparently there is a shift of the absorption onset at the wavelengths of ~ 400–500 nm.

OSA CONTINUUM

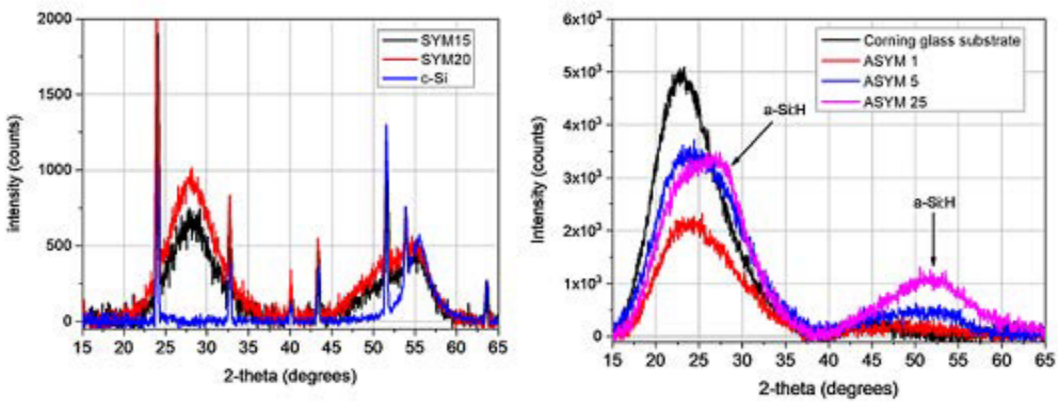

Fig. 3. XRD patterns of SYM samples (left) recorded on the identical samples deposited on c-Si substrate and ASYM samples (right) on Corning glass substrate. Sharp lines (left) correspond to Laue peaks stemming from the substrate and coincide with XRD pattern of c-Si.

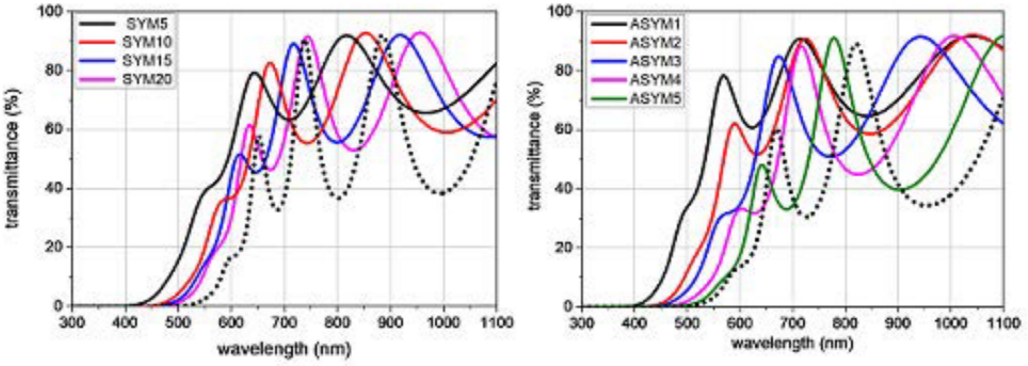

Fig. 4. Optical transmittances of SYM (left) and ASYM (right) samples. For the comparison the transmittance of a single a-Si:H thin films deposited at $R = 0$ (~ 400 nm left [22])) and (~ 300 nm right [23] included (short dot).

OSA CONTINUUM

3. Optical properties

3.1. Theoretical background

Reflection and transmission of light from a ML structure bound on either side by semi-infinite substrate is usually calculated by transfer matrix or transmission line methods. However in subwavelength structures where the thicknesses of individual sublayers are much smaller than the wavelength of light, it is generally agreed that a normally directed light wave interacts with the multilayer as a whole. Then the structure can be seen as homogeneous characterized by effective parameters [26–28]. Therefore our model was based on the consideration of a ML as a homogeneous slab with parallel interfaces and effective optical properties. This approach enables neglecting the surface and interface internal imperfections if they are much smaller than the total ML thickness.

Due to weak absorption of light above the absorption edge at the wavelengths > 500 nm apparent interference fringes are present in spectra (Fig. 4). As their wavelength position, spacing and transmittance depend on optical properties of the effective thin film and the film thickness, transmittance spectra differ. Due to the dispersion, i.e. the dependence of the refractive index and the extinction coefficient on the wavelength, interference extrema are not equidistant. The transmittance in interference maxima (positive interference) increases as the absorption of the thin film material decreases. If the thickness of all ML samples within one series is comparable, the differences in transmittance spectra of the individual samples are caused by different optical properties. The change of optical properties is mainly due to the varying amount of a-Si:H and a-SiN_x:H constituents in the final effective slab.

The optical transmittance of a homogeneous thin film with parallel interfaces deposited on a thick substrate is a nonlinear function of the wavelength, the film thickness and the complex refractive index $N = n + ik$ of the film and the substrate (the refractive index n and the extinction coefficient k) [29]. We extracted the wavelength-dependent n, k from measured transmittance spectra in Fig. 4 using a global optimization procedure. The optimization was based on genetic algorithm under considering the ML structure as one effective thin film. The optimization procedure minimized differences between the experimental and theoretical transmittance in the broad spectral region including the region in the vicinity of the absorption edge. The theoretical transmittance was calculated using the theory in [29] and the Tauc-Lorentz dispersion model for the dependence of n, k on the wavelength [30]. As the transmittance depends also on the total ML thickness, this value belongs to optimization procedure parameters that can be determined from fitting the transmittance spectrum (Table 1, Table 2). In Fig. 5 there is comparison of experimental and theoretical curves of two multilayers as an example. The differences in interference maxima in the vicinity of ~ 800 nm probably stem from neglecting the surface and interface roughness in the theoretical model.

3.2. Absorption coefficients and optical band gaps

Figure 6 shows the absorption coefficients α related to k and the wavelength λ as $\alpha = 4\pi k/\lambda$ depicted versus the photon energy. High absorption coefficients (> 10^5 cm^{-1}) are achieved at photon energies > 2.8 eV (λ < 450 nm) for both series of multilayers. Still it is obvious that the slopes of the characteristics differ what means differences in optical band gaps. The differences of the absorption coefficients of ASYM structures at photon energies < 2 eV are obviously more pronounced than those of SYM structures.

As a result of the partial disorder in amorphous a-Si:H and a-SiN_x:H, the band edges are extended and the tail states play important role in optical and electronic properties. Therefore it is quite puzzling to determine optical bandgaps E_g^{opt} from optical measurements only without some ambiguities. The widely adopted procedure is the so-called Tauc plot of $(\alpha E)^{1/2}$ versus the photon energy E. The plot leads to a straight line whose intersection with the E-axis gives E_g^{opt}.

OSA CONTINUUM

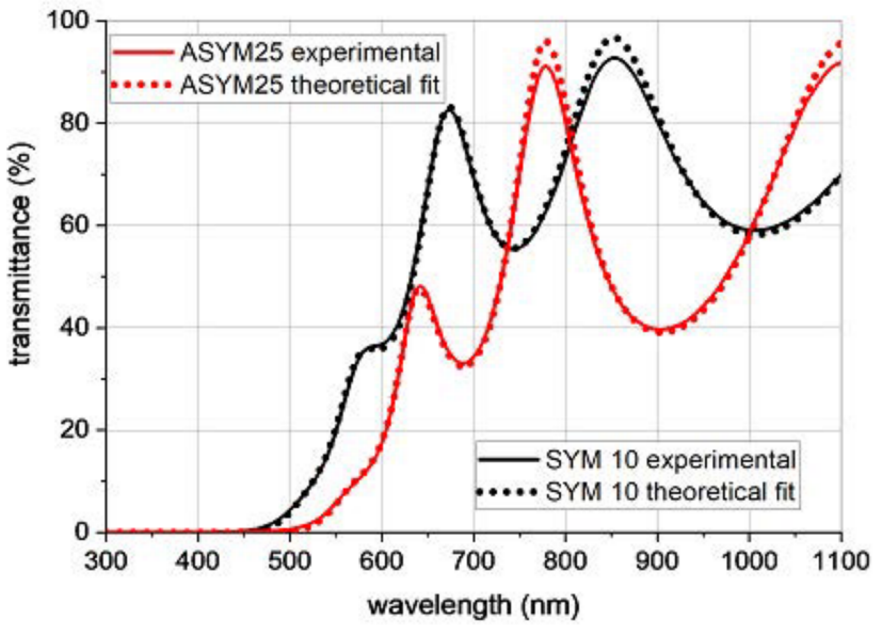

Fig. 5. The comparison of experimental and theoretical transmittances.

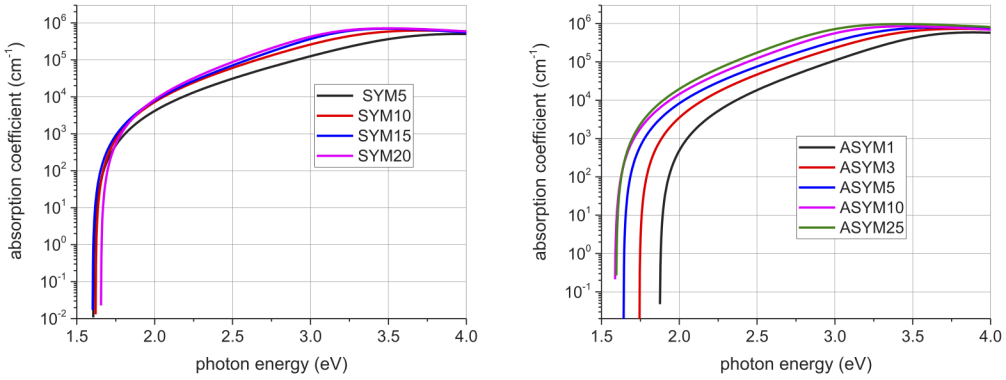

Fig. 6. Absorption coefficients of SYM (left) and ASYM (right) samples.

OSA CONTINUUM

An alternative way to characterize the optical band gap is the iso-absorption gap E_{04} defining the photon energy, at which the absorption coefficient achieves the value of 10^4 cm^{-1}. Although not reflecting particular differences in optical absorption, E_{04} is tolerable when the linear part of $(\alpha E)^{1/2}$ plot versus E is reduced. Here the values of E_{04} are well distinguished for both series. E_g^{opt} and E_{04} are listed in Table 3.

Table 3. Comparison of optical properties of SYM and ASYM samples: Tauc optical band gap E_g^{opt}, iso-absorption gap E_{04}, refractive index in the long-wavelength limit n_∞, the Yablonovitch limit $4n_\infty^2$ and solar spectrum absorptance A_{solar}.

	SYM						ASYM				
	E_g^{opt} (eV)	E_{04} (eV)	n_∞	$4n_\infty^2$	A_{solar}		E_g^{opt} (eV)	E_{04} (eV)	n_∞	$4n_\infty^2$	A_{solar}
5	2.40	2.18	2.345	22.00	0.549	**1**	2.11	2.37	2.427	23.51	0.412
10	2.30	2.06	2.565	26.32	0.581	**3**	2.09	2.15	2.600	27.04	0.508
15	2.29	2.05	2.611	27.27	0.595	**5**	2.06	2.03	2.843	32.33	0.576
20	2.26	2.03	2.720	29.59	0.582	**10**	2.04	1.94	3.109	38.66	0.621
						25	2.00	1.89	3.382	45.75	0.635

Due to the presence of wide-band-gap a-SiN$_x$:H, optical band gaps of multilayers are higher than 1.7–1.9 eV that are usually reported for a-Si:H thin film of various hydrogen content and thickness [28,31,32]. Therefore the multilayers of this kind can conveniently serve as upper high band gap cell in tandem solar cells in which tuning the band gap is welcome. Moreover we observe that with decreasing thickness of a-Si:H layers, the Tauc optical band gap increases, i.e. blueshift occurs. This increment can be attributed to the quantum confinement effect in thinner sublayers.

3.3. *Refractive indices*

Refractive index spectra are in Fig. 7 for SYM samples (left) and ASYM samples (right).

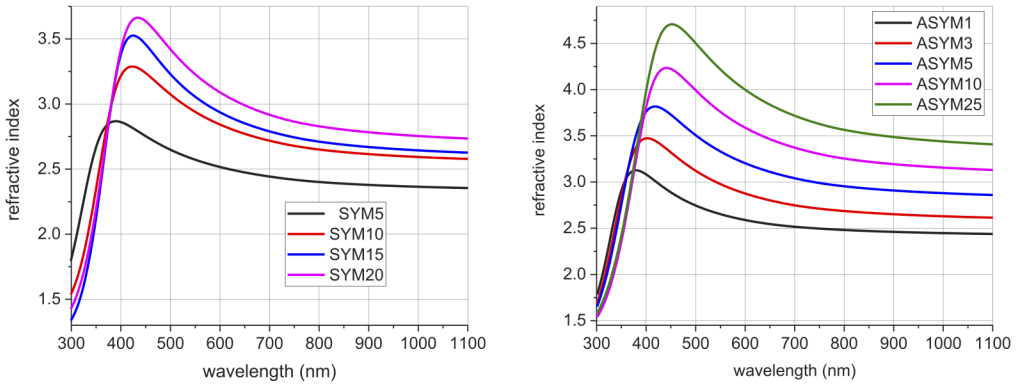

Fig. 7. Refractive indices of SYM (left) and ASYM samples (right).

Due to mixing with a-SiN$_x$:H, the refractive indices n of all multilayers are lower than those for standard undiluted a-Si:H [32–34]. The changes are more pronounced in case of ASYM samples, in which the increasing amount of high-index a-Si:H in the structure induces the increase of the refractive index. In SYM samples the amount of a-Si:H and a-SiN$_x$:H differs only by one capping a-SiN$_x$:H sublayer. Here the differences in the refractive indices must be caused by additional agent, most probably by the presence of voids or vacancies in the amorphous structure. As we found out in the past, the porosity of a-Si:H deposited from (SiH_4+H_2) mixture using

OSA CONTINUUM

Ar is higher than that deposited from (SiH_4+H_2) without Ar [24]. This must be the reason of a lower refractive index. However a good message is the possibility to engineer the refractive index, i.e. the reflection loss of solar light impinging the stack and the Yablonovitch limit $4n^2$ by a specific design of a multilayer as can be seen in Table 3.

Extrapolating n to the non-absorbing region (extinction coefficients $k \rightarrow 0$), the so-called refractive indices n_∞ in the long-wavelength limit were resolved as important optical parameters related to the mass density (Table 3). For both series they obviously increase with increasing thickness of a-Si:H sublayers indicating increasing material density.

3.4. Solar absorptance under the Yablonovitch limit

The knowledge of the wavelength-dependent absorption coefficient $\alpha(\lambda)$ (Fig. 6) and the refractive index $n(\lambda)$ (Fig. 7) is important for the structure optical characterization. However for the photon harvesting they must be considered complex. It is known that absorption enhancement can be achieved by the increase of optical path in an absorbing material via proper light-trapping schemes such as surface/interface texturization. The Yablonovitch absorptance serves as a benchmark that can be theoretically achieved by an absorbing material. The absorptance in the Yablonovitch limit assumes perfect antireflection and perfect Lambertian light trapping with a limiting path length enhancement of $4n^2$[35–38]. It can be used to consider the light trapping limit, e.g. in sensing, photodecting or photovoltaic applications.

Multiple interfaces in an ML structure can act as light trapping agents due to multiple reflections. Knowing $\alpha(\lambda), n(\lambda)$ of an ML structure regarded as an effective single homogeneous thin film with parallel and smooth interfaces, we can calculate the absorptance $A(\lambda)$ in the Yablonovitch limit as

$$A(\lambda) = \frac{\alpha(\lambda)d}{\alpha(\lambda)d + \frac{1}{F}} = \frac{\alpha(\lambda)d}{1 + \frac{1}{4n^2(\lambda)d}} \tag{1}$$

where d is the overall ML thickness and $F = 4n^2$ is the absorption enhancement factor. This approximation is often used to consider maximization of light absorption in optoelectronic devices, e.g. solar cell or photodiodes.

The Yablonovitch absorptance $A(\lambda)$ predicted for ML as effective thin films can be seen in Fig. 8. In calculations we use the values of d from the experimental transmittance analysis (Tables 1 and 2). The achieved differences can be clearly seen. The absorbed light increases with the number of layers (SYM) or with the thickness of a-Si:H layers corresponding to the amount of a-Si:H. However the absorptance achieved with a ML structure is higher than that for a single a-Si:H thin film deposited under comparable conditions and of similar thickness (Fig. 8).

In spite of the fact that the Yablonovitch absorptance is calculated as an ideal theoretical limit, the obtained values confirm its ability to reflect differences in individual members of the series SYM and ASYM and their absorbing strengths. We conclude that a specific design of a ML structure has potential to increase the solar absorptance and therefore to improve the solar cell efficiency only via absorber concept and without special texturization similarly as in [39]. Here the solar absorptance enhancement is obvious and can be tuned by adjusting the a-Si:H layer thickness. Similar improvements were reported for Si/SiO_2 multilayers using annealing and adjusting the Si layer thickness [40].

Although the SYM and ASYM series were not deposited under exactly identical PECVD deposition conditions, a general conclusion concerning $A(\lambda)$ could be accepted. The absorptance $A(\lambda)$ enhancements are better pronounced in case of ASYM samples with thinner (and constant for all member of the series) barrier sublayer of a-SiN_x:H. The increase of the Yablonovitch absorptance with increasing the thickness of a-Si:H sublayer up to 10 nm is remarkable. The difference of $A(\lambda)$ of ASYM10 and ASYM25 sample seems to be less apparent. Therefore we deduce that ASYM multilayers with a thin and constant a-SiN_x:H sublayer and optimized

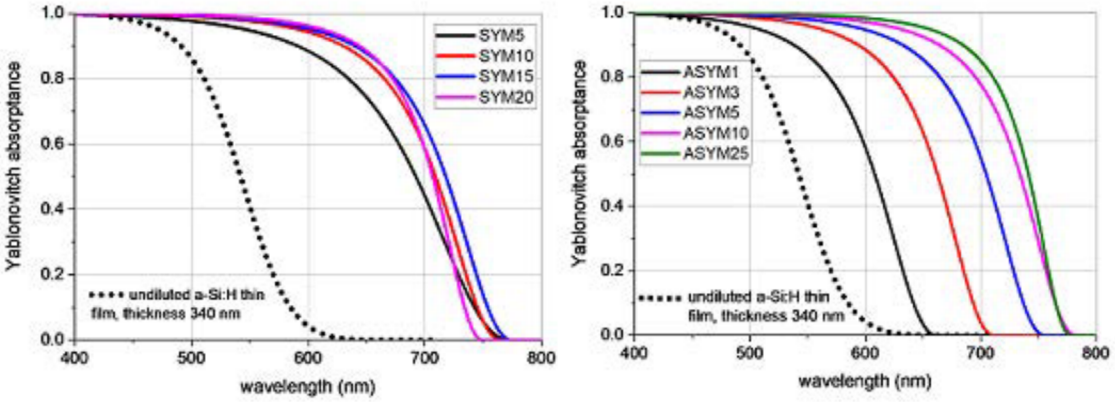

Fig. 8. Yablonovitch absorptance of SYM (left) and ASYM (right) samples. Yablonovitch absorptance (short dot line) calculated for undiluted a-Si:H thin film of the thickness of 340 nm similar to overall thickness of ASYM25 sample added for the comparison (data of $\alpha(\lambda)$, $n(\lambda)$ from [32]).

of a-Si:H sublayer thickness are more suitable for absorption related applications, such as photovoltaics, light sensors, photodetectors etc.

A merit of the suitability of a-Si:H/a-SiN_x:H multilayers as solar cell absorbers is the total relative integrated absorptance

$$A_{solar} = \frac{\int_{\lambda_1}^{\lambda_2} A(\lambda) S_{\mathrm{AM1.5g}}(\lambda) d\lambda}{\int_{\lambda_1}^{\lambda_2} \mathrm{S}_{\mathrm{AM1.5g}}(\lambda) d\lambda} \tag{2}$$

In this equation $S_{\mathrm{AM1.5g}}$ is the AM1.5 reference solar global spectral irradiance from ASTM G173-03 [41]. Figure 9 illustrates the influence of specific ASYM design on the spectrum of $A(\lambda)S_{\mathrm{AM1.5g}}(\lambda)$ that is related to the spectral solar global irradiance absorbed by the sample.

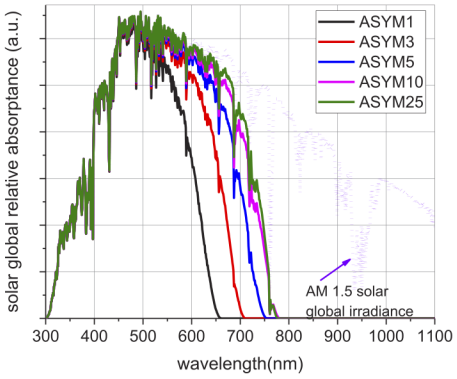

Fig. 9. The absorptance of solar global spectral irradiance by ASYM samples. AM 1.5 solar global irradiance is included for comparison.

A_{solar} declares the relative solar irradiance absorbed by the sample. This figure is proportional to the photogenerated current density of a solar cell and therefore could directly affect the solar cell efficiency. The values of A_{solar} in Table 3 calculated according to Eq. (2) show the increase

OSA CONTINUUM

with increasing thickness of a-Si:H sublayers. The wavelength range of interest in the integration in Eq. (2) is limited to the optical properties analysis (λ_1 = 300 nm, λ_2 = 1100 nm). The growth of A_{solar} in ASYM samples clearly corresponds to the increasing amount of a-Si:H although the increase of A_{solar} between ASYM10 and ASYM25 is less apparent. In SYM samples a certain growth attributed to the thickness effect can be seen, too.

It is obvious, that when using such absorbers is solar cells, additional studies related to the thickness of a-SiN_x:H barrier sublayers and the carrier transport through interfaces of ML structures are necessary. As reported in [11] a-SiN_x:H barrier layers thicker than several nm may prevent charge carrier transport to electrodes in solar cells.

4. Conclusions

In this paper a study of effective optical properties of two series of differently arranged PECVD deposited planar a-Si:H/a-SiN_x:H multilayers was presented. Layers arranged in symmetric or asymmetric design resulted in changes of the transmittance spectra, from which effective refractive indices, absorption coefficients and optical band gaps were extracted and compared. With increasing thickness of a-Si:H layer the refractive index increases representing denser effective material. Optical band gaps are found to be decreasing function of the thickness of a-Si:H layer. In general, observed differences in optical properties are more pronounced for ASYM samples. The importance of knowledge of wavelength-dependent refractive indices and absorption coefficients was demonstrated in the calculations of the spectral absorptance under the Yablonovitch limit and the total relative absorbed solar irradiance that can be related to the solar cell performance. The results indicate that a specific a-Si:H/a-SiN_x:H multilayer design can influence significantly the absorptance of solar light and improve an a-Si:H/a-SiN_x:H multilayer solar absorber in comparison with a single a-Si:H thin film absorber of a comparable thickness. We recommend ASYM concept with thin a-SiN_x:H sublayers of the constant thickness that offers more pronounced effect on optical properties (refractive index, absorption coefficient, optical band gap) and solar absorptance. Within ASYM concept the thickness of a-Si:H sublayers should be optimized.

Funding

Agentúra na Podporu Výskumu a Vývoja (APVV-15-0152, APVV-17-0631); Vedecká Grantová Agentúra MŠVVaŠ SR a SAV (VEGA 1/0840/18); Ministerstvo Školství, Mládeže a Tělovýchovy (CENTEM CZ.1.05/2.1.03.0088, CENTEM+(LO1402)).

Acknowledgments

Prof. M. Zeman and Dr. S.M. Luxembourg from the Delft University of Technology, the Netherlands, are acknowledged for the deposition of ASYM samples.

Disclosures

The authors declare no conflicts of interest.

References

1. Q. Wilmart, H. El Dirani, N. Tyler, D. Fowler, S. Malhouitre, S. Garcia, M. Casale, S. Kerdiles, K. Hassan, C. Monat, X. Letartre, A. Kamel, M. Pu, K. Yvind, L. K. Oxenløwe, W. Rabaud, C. Sciancalepore, B. Szelag, and S. Olivier, "A versatile silicon-silicon nitride photonics platform for enhanced functionalities and applications," Appl. Sci. **9**(2), 255 (2019).
2. C. Song, R. Huang, X. Wang, Y. Guo, and J. Song, "Tunable red light emission from a-Si:H/a-SiN multilayers," Opt. Mater. Express **3**(5), 664–670 (2013).
3. M. S. D. Zan, I. Kato, M. S. Ab-Rahman, and S. M. Mestaza, "Characterization of a-Si:H/SiN multilayer waveguide polarization using an optical pumping application—LED," J. Zhejiang Univ., Sci., A **10**(10), 1421–1427 (2009).

OSA CONTINUUM

4. R. S. Dubey, K. Jhansirani, and S. Singh, "Investigation of solar cell performance using multilayer thin film structure (SiO_2/Si_3N_4) and grating," Results Phys. **7**, 77–81 (2017).
5. J. C. C. Mak, W. D. Sacher, H. Ying, X. Luo, P. G.-Q. Lo, and J. K. S. Poon, "Multi-layer silicon nitride-on-silicon polarization-independent grating couplers," Opt. Express **26**(23), 30623–30633 (2018).
6. O. Isabella, R. Vismara, A. Ingenito, N. Rezaei, and M. Zeman, "Decoupled front/back dielectric textures for flat ultra-thin c-Si solar cells," Opt. Express **24**(6), A708–A719 (2016).
7. H. J. El-Khozondar, R. J. El-Khozondar, M. M. Shabat, and D. M. Schaadt, "Solar cell with multilayer structure based on nanoparticles composite," Optik **166**, 127–131 (2018).
8. A. K. Panchal, D. K. Rai, M. Mathew, and C. S. Solanki, "a-Si/SiN multilayered light absorber for solar cell," J. Nanopart. Res. **13**(6), 2469–2473 (2011).
9. M. Zeman, O. Isabella, K. Jäger, R. Santbergen, S. Solntsev, M. Topic, and J. Krc, "Advanced Light Management Approaches for Thin-Film Silicon Solar Cells," Energy Procedia **15**, 189–199 (2012).
10. C. Ricciardi, V. Ballarini, M. Galli, M. Liscidini, L. C. Andreani, M. Losurdo, G. Bruno, S. Lettieri, F. Gesuele, P. Maddalena, and F. Giorgis, "Amorphous silicon nitride: a suitable alloy for optical multilayered structures," J. Non-Cryst. Solids **352**(9-20), 1294–1297 (2006).
11. M. Zeman, O. Isabella, F. D. Tichelaar, and S. L. Luxembourg, "Amorphous silicon-based multilayers for photovoltaic applications," Phys. Status Solidi C **7**(3-4), 1057–1060 (2010).
12. A. Fosca, A. Slaoui, H. Charifi, J. P. Stoquert, and S. Roques, "Surface passivation at low temperature of p- and n-type silicon wafers using a double layer a-Si:H/SiNx:H," Mater. Sci. Eng., B **159-160**, 242–247 (2009).
13. D. Callahan, K. A. W. Horowitz, and H. A. Atwater, "Light trapping in ultrathin silicon photonic crystal superlattices with randomly-textured dielectric incouplers," Opt. Express **21**(25), 30315 (2013).
14. S. Abdelatif, K. Kirah, R. Ghannam, A. S. G. Khalil, and W. Anis, "Enhancing the absorption capabilities of thin-film solar cells using sandwiched light trapping structures," Appl. Opt. **54**(17), 5534–5541 (2015).
15. M. Burresi, F. Pratesi, F. Roboli, and D. S. Wiersma, "Complex photonic structures for light harvesting," Adv. Opt. Mater. **3**(6), 722–743 (2015).
16. E. Yablonovitch and G. D. Cody, "Intensity enhancement in textured optical sheets for solar-cells," IEEE Trans. Electron Devices **29**(2), 300–305 (1982).
17. S. J. Fonash, "Introduction to Light Trapping in Solar Cell and Photo-detector", first ed., Academic Press as an imprint of Elsevier, 2015.
18. M. Lamers, K. Butler, P. E. Vullum, J. Harding, and A. Weeber, "Characterization of a-SiN:H layer: Bulk properties, interface with Si and solar cell efficiency," Phys. Stat. Sol. A **210**(4), 658–668 (2013).
19. H. Ghosh, S. Mitra, H. Saha, S. K. Datta, and C. Banerjee, "Argon plasma treatment of silicon nitride (SiN) for improved antireflection coating on c-Si solar cells," Mater. Sci. Eng., B **215**, 29–36 (2017).
20. I. Guler, "Optical and structural characterization of silicon nitride thin films deposited by PECVD," Mater. Sci. Eng., B **246**, 21–26 (2019).
21. P. Šutta, P. Calta, J. Müllerová, M. Netrvalová, R. Medlín, J. Savková, and V. Vavruňková, "Transition from a-Si:H to Si_3N_4 in thin films deposited by PECVD technology from silane diluted with nitrogen," *IEEE Proc. 10th International Conference on Advanced Semiconductor Devices and Microsystems ASDAM 2014*, ISBN 978-1-4799-5474-2, 4 pages, (2014).
22. J.-F. Lelièvre, E. Fourmond, A. Kaminski, O. Palais, D. Ballutaud, and M. Lemiti, "Study of the composition of hydrogenated silicon nitride SiNx:H for efficient surface and bulk passivation of silicon," Sol. Energy Mater. Sol. Cells **93**(8), 1281–1289 (2009).
23. P. Calta, P. Šutta, R. Medlín, and M. Netrvalová, "Impact of sublayer thickness and annealing on silicon nanostructures formation in a-Si:H/a-SiN:H superlattices for photovoltaics," Vacuum **153**, 154–161 (2018).
24. J. Müllerová, P. Šutta, L. Prušáková, and M. Netrvalová, "Dispersive and BEMA investigation on optical properties of photovoltaic thin films," Proc. SPIE **9441**, 94411J (2014).
25. J. Müllerová, V. Vavruňková, P. Šutta, and R. Srnánek, "Microstructure related optical characterization of technologically relevant hydrogenated silicon thin films," Proc. SPIE **7141**, 714103 (2008).
26. S. V. Zhukovsky, A. Andryieuski, O. Takayama, E. Shkondin, R. Malureanu, F. Jensen, and A. V. Lavrinenko, "Experimental demonstration of effective medium approximation breakdown in deeply subwavelength all-dielectric multilayers," Phys. Rev. Lett. **115**(17), 177402 (2015).
27. C. R. Simovski, "On electromagnetic characterization and homogenization of nanostructured metamaterials," J. Opt. **13**(1), 013001 (2011).
28. H. H. Sheinfux, I. Kaminer, Y. Plotnik, G. Bartal, and M. Segev, "Subwavelength multilayer dielectrics: Ultrasensitive transmission and breakdown of effective-medium theory," Phys. Rev. Lett. **113**(24), 243901 (2014).
29. J. Müllerová and P. Šutta, "On some ambiguities of the absorption edge and optical band gaps of amorphous and polycrystalline semiconductors," Communications **19**(3), 9–15 (2017).
30. G. E. Jellison Jr. and F. A. Modine, "Parametrization of the optical functions of amorphous materials in the interband region," Appl. Phys. Lett. **69**(3), 371–373 (1996) and erratum Appl. Phys. Lett. **69**, 2137 (1996).
31. T. M. Mok and S. K. O'Leary, "The dependence of the Tauc and Cody optical gaps associated with hydrogenated amorphous silicon on the film thickness: αl Experimental limitations and the impact of curvature in the Tauc and Cody plots," J. Appl. Phys. **102**(11), 113525 (2007).

OSA CONTINUUM

32. J. Müllerová, V. Vavruňková, and P. Šutta, "Optical absorption in PECVD deposited thin hydrogenated silicon in light of ordering effects," Cent. Eur. J. Phys. **7**(2), 315–320 (2009).
33. J. Müllerová, L. Prušáková, M. Netrvalová, V. Vavruňková, and P. Šutta, "A study of optical absorption in amorphous hydrogenated silicon thin films of varied thickness," Appl. Surf. Sci. **256**(18), 5667–5671 (2010).
34. A. S. Ferlauto, G. M. Ferreira, J. M. Pearce, C. R. Wronski, R. W. Collins, X. Deng, and G. Ganguly, "Analytical model for the optical functions of amorphous semiconductors from the near-infrared to ultraviolet: Applications in thin film photovoltaics," J. Appl. Phys. **92**(5), 2424–2436 (2002).
35. M. A. Green, "Lambertian light trapping in textured solar cells and light-emitting diodes: Analytical Solutions," Prog. Photovolt: Res. Appl. **10**(4), 235–241 (2002).
36. K. X. Wang, Z. Yu, V. Liu, Y. Cui, and S. Fan, "Absorption Enhancement in Ultrathin Crystalline Silicon Solar Cells with Antireflection and Light-Trapping Nanocone Gratings," Nano Lett. **12**(3), 1616–1619 (2012).
37. A. Ingenito, O. Isabella, and M. Zeman, "Experimental demonstration of $4n^2$ classical absorption limit in nanotextured ultrathin solar cells with dielectric omnidirectional back reflector," ACS Photonics **1**(3), 270–278 (2014).
38. L. A. Weinstein, W.-C. Hsu, S. Yerci, S. V. Boriskina, and G. Chen, "Enhanced absorption of thin-film photovoltaic cells using optical cavity," J. Opt. **17**(5), 055901 (2015).
39. X. Ziang, L. Shifeng, Q. Laixiang, P. Shuping, W. We, Y. Yu, Y. Li, C. Zhijian, W. Shufeng, D. Honglin, Y. Minghui, and G. G. Qin, "Refractive index and extinction coefficient of CH3NH3PbI3 studied by spectroscopic ellipsometry," Opt. Mater. Express **5**(1), 29–43 (2015).
40. S. Yamada, M. Konagai, and S. Miyajima, "Investigation of the optical absorption in Si/SiO_2 superlattice for the application to solar cells," Jpn. J. Appl. Phys. **55**(4S), 04ES06 (2016).
41. ASTM Standard Tables for Reference Solar Spectral Irradiances, Standard G173-03 (2012), American Society for Testing and Materials, Philadelphia, PA.